Optimized Cross-Polarized LEKIDs for *W*-Band Using Sawtooth Inductors

Marina C. de Ory, David Rodriguez, Enrique Villa, Luisa de la Fuente, *Member, IEEE*, Beatriz Aja, Victor Rollano, María Teresa Magaz, Juan P. Pascual, *Senior Member, IEEE*, Daniel Granados, Eduardo Artal, *Life Member, IEEE*, and Alicia Gomez

***Abstract*— Lumped-element kinetic inductance detectors (LEKIDs) based on sawtooth inductors for *W*-band are presented in this article. A careful analysis is carried out for the cross-polarization in the inductor geometry, which brings out the absorption of the nondesired *E*-field component of an incident wave plane. The proposed inductor geometry with sawtooth sections demonstrates improved cross-polarization. The analytical results are verified by comparison with 3-D electromagnetic (EM) simulations. As the first proof of concept, *W*-band optical response is demonstrated through quasioptical characterization at room temperature of an aluminum LEKID array. Moreover, a LEKID array based on bilayer superconducting titanium/aluminum (Ti/Al) thin film is developed for evaluating the performance at millikelvin temperatures. Darkness characterization confirms the high-quality factor of the fabricated detectors and the low-frequency design reliability. In addition, cryogenic optical experiments are performed for spectroscopic and detector sensitivity characterization. The proposed geometry opens the possibility of developing large-format polarimetric cameras based on on-chip LEKID structures for future astronomical experiments.**

***Index Terms*— Cryogenics, kinetic inductance detector (KID), lumped-element resonator, millimeter-wave astronomy, polarimeter, superconducting microwave devices.**

Manuscript received 11 July 2023; revised 18 September 2023 and 13 November 2023; accepted 14 November 2023. Date of publication 28 November 2023; date of current version 10 January 2024. This work was supported in part by the Centro de Astrobiología and IMDEA-Nanociencia under Grant PID2019-105552RBC41 and Grant PID2019-105552RB-C44, in part by the Comunidad de Madrid under Grant P2018/NMT-4291 TEC2SPACE-CM, in part by the "Severo Ochoa" Programme for Centers of Excellence in Research and Development under Grant SEV-2016-0686, in part by the CSIC Research Platform under Grant PTI-001, and in part by the Comunidad de Madrid, the Recovery, Transformation and Resilience Plan from the Spanish State, and NextGenerationEU from the EU Recovery and Resilience Facility through the Project "Tecnologías avanzadas para la exploración del Universo y sus componentes" under Grant PR47/21 TAU-CM. The work of Universidad de Cantabria was supported by the Ministry of Science and Innovation under Grant PID2019 110610RB-C22. All groups were partially funded by the Research Network under Grant RED2022-134839-T. This article is an expanded version of the IEEE MTT-S International Microwave Symposium (IMS 2023). *(Corresponding author: Alicia Gomez.)*

Marina C. de Ory, David Rodriguez, Enrique Villa, María Teresa Magaz, and Alicia Gomez are with the Centro de Astrobiología (CSIC-INTA), 28850 Madrid, Spain (e-mail: mcalero@cab.inta-csic.es; agomez@cab.inta-csic.es).

Luisa de la Fuente, Beatriz Aja, Juan P. Pascual, and Eduardo Artal are with the Dpto. Ing. Comunicaciones, Universidad de Cantabria, 39005 Santander, Spain.

Victor Rollano is with the Departamento de Física de la Materia Condensada and the Instituto de Nanociencia de Aragón, CSIC-Universidad de Zaragoza, 50009 Zaragoza, Spain, and also with the Hefei National Laboratory for Physical Sciences at the Microscale, University of Science and Technology of China, Hefei 230026, China.

Daniel Granados is with IMDEA-Nanociencia, 28049 Madrid, Spain.

Color versions of one or more figures in this article are available at https://doi.org/10.1109/TMTT.2023.3334816.

Digital Object Identifier 10.1109/TMTT.2023.3334816

I. Introduction

SPACE- or ground-based experiments increasingly require improved detectors, in terms of responsivity or noise performance, to reach new scientific milestones. In this regard, applications such as radio astronomy in the investigation of the origin of the Universe or the detection of dark matter [1] are continuously demanding state-of-the-art detectors able to distinguish extremely low-power signals. However, there is also a great interest in detecting the polarization of the incoming radiation. Particularly, the characterization of the polarization of the cosmic microwave background (CMB) radiation is considered to bring crucial information about the early stages of the Universe such as the epoch of reionization and the inflation time [2], [3], [4].

In the last years, low-temperature detectors have significantly evolved, providing significant roles in scientific applications at subKelvin temperatures [5], [6]. These detectors employ superconducting materials to substantially improve detection limits and they have demonstrated significant results in terms of sensitivity within millimeter-wave bands [7], [8]. Among superconducting detectors, kinetic inductance detectors (KIDs) are of particular interest since they are inherently multiplexable in the frequency domain, which enables the use of thousands of detectors over a single readout line [9].

KIDs are being employed in many radio astronomy instruments for millimeter and submillimeter-wave applications with thousands of multiplexed detectors [10], [11], [12], [13], [14]. Two main types of KIDs are defined depending on how they absorb the radiation: antenna-coupled microwave KIDs (MKIDs) [15] and lumped-element KIDs (LEKIDs) [16]. LEKIDs consist of a discrete meandered inductor in series with an interdigital capacitance coupled to a single transmission line. In comparison with MKIDs that use quarter-wavelength resonators, LEKIDs are more sensitive as a high and constant current density distribution is achieved in the lumped element inductor at resonance conditions.

Applications such as CMB experiments have pushed forward the development of new LEKID designs, focused on improving their sensitivity at lower-frequency bands, such as the *W*-band, and simultaneously developing dual-polarization designs [17], [18], [19]. Furthermore, LEKID designs based on Hilbert fractal structures were implemented to evaluate polarization sensitivity, taking advantage of the use of a single layer for absorbing both orthogonal polarizations [13]. However, this option requires duplicating the number of arrays and using an external polarizer. Other experiments proposed the detection of polarization by using KIDs together with an orthomode transducer (OMT), which separates orthogonal components of the polarized signal [20], [21]. LEKIDs have demonstrated significant results in being able to absorb orthogonal polarizations, but at higher-frequency bands [12], [22]. However, this performance has not been demonstrated at the W-band yet.

Aja et al. [23] proposed a W-band on-chip polarimeter based on two LEKIDs that consist of a series capacitor–inductor resonator coupled to a single 50-Ω coplanar waveguide (CPW) transmission line. They are stacked one on top of the other and placed in orthogonal directions. This proposal is of particular interest since a minimum value of the foreground contamination is reached in this frequency range, thus a great effort is being made in the development of suitable W-band detectors [2]. However, de Ory et al. [24] showed an extra cross-polarization that prevents its good performance as a polarimeter. Hence, in this work, we aim to minimize this cross-polarization. A new design is proposed based on sawtooth inductors to enhance LEKIDs performance in a single polarization to develop an optimized on-chip polarimeter for the W-band.

The article is organized as follows. After the Introduction, Section II describes high- and low-frequency designs of the LEKIDs for operation at the W-band. Section III deals with the tuning of the cut-off frequency of the superconductor based on titanium/aluminum (Ti/Al), describing the proposed methodology and fabrication. Section IV presents experimental set-ups to perform room temperature and cryogenic tests, describing the prototype assemblies. Test results at room and cryogenic temperatures are detailed in Section V. Finally, Section VI presents conclusions summarizing this article.

II. W-Band LEKID Design

The detector's design involves two steps: on the one side, the inductor improvement, in which geometry and impedance determine the absorption efficiency and responsivity; on the other side, the low-frequency design, including capacitor dimensions and electrical coupling, which determines its quality factor and resonant frequency, critical parameters for the LEKIDs readout. In Sections II-A and II-B, both steps are described.

A. W-Band Coupling Design

In LEKIDs, the inductor acts as the sensitive part of the detector, so a careful analysis of its geometry is critical for obtaining optical impedance matching and, therefore, optimizing the optical response. The traditional LEKID design, as described in [25] and shown in Fig. 1(a), is composed of long vertical strips that are addressed for providing the maximum absorption for a vertical E-field. These vertical inductor sections are joined by short horizontal lines, required to build the necessary inductance for the low-frequency resonator and to allow current flow. As a consequence of their orthogonal direction to the desired E-field radiation, these short lines have a nonnegligible impact and cause a nondesired absorption of the orthogonal E-field component, which produces a cross-polarization effect.

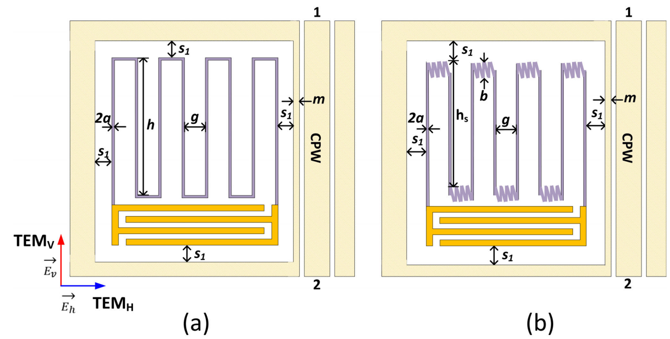

Fig. 1. Structure of LEKIDs. A meander inductor with strips of width $2a$ and spacing g. Coupling separation (s_1 and m) between the resonator and the readout 50-Ω CPW feedline. (a) Inductor with straight short horizontal stripes [24]. (b) Inductor with sawtooth horizontal strips.

To reduce the cross-polarization effect, the sensitivity to the orthogonal E-field needs to be minimized. This can be done by modifying the horizontal section's impedance, diminishing the absorption of the undesired polarization. A circuit model is developed for analyzing the impedance of different geometries, to understand the origin of this undesired absorption. Although more accurate results are obtained through 3-D electromagnetic (EM) simulations, this previous development of the equivalent circuit models is very useful for optimizing the LEKID design and its response.

Several types of sections, such as wiggled sections [12], triangular shapes, or sawtooth shape lines, are analyzed in terms of the input impedance of a periodic array. An improved structure based on a sawtooth shape is proposed, where small vertical lines joined by angled ones replace the short horizontal sections [see Fig. 1(b)]. The smaller angle with shorter distances between vertical short sections provides a higher reflection coefficient in the structure, minimizing the absorption of the orthogonal incident E-field. The best results, compatible with the nanofabrication process, are obtained for the sawtooth shape with short vertical strips joined with lines at 15° angle. An additional advantage of this modification is that it also increases the inductor volume and, then, the dynamic range of the detector [12].

To understand the optical matching of this configuration, an incident wave with vertical E-field (TEM_V) referred to the position of the LEKID in Fig. 1 is considered. Because the long sections in both Fig. 1(a) and (b) have the same geometry ($2a$, g), they present the same impedance, with a resistive part and an inductive reactance. The impedance for this parallel metal strip grating is obtained based on equations in [26], [27], which are valid for spacing between strips shorter than λ. On the other hand, the short sections of the meandered line cause a capacitive reactance. The calculation of the impedance for these short horizontal sections is performed using a

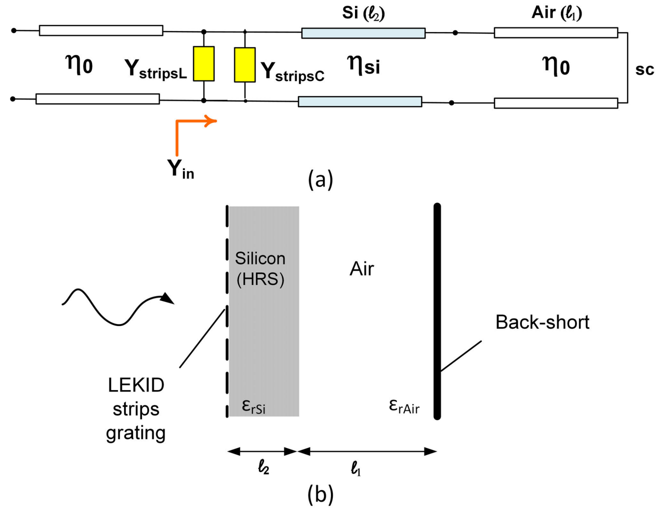

Fig. 2. (a) Equivalent circuit with transmission lines of an LEKID with the structure to be optically matched to the free space. (b) Cross section of a single-polarization LEKID.

complete expression described in [26, Secs. 5–19, eq. (1a)]. In both cases, metal strips have an inductive behavior for an electrical field parallel to them, Y_{stripsL}, and a capacitive behavior for an orthogonal electrical field, Y_{stripsC}. This capacitive effect is very small and practically negligible for the transmission of a so-oriented EM wave component.

The proposed circuit based on transmission lines is shown in Fig. 2(a), where η_0 is 377 Ω, $\varepsilon_{r\text{Si}} = 11.9$, and $\eta_{\text{Si}} = \eta_0/(\varepsilon_{r\text{Si}})^{1/2}$ is 109.29 Ω. This circuit also includes the silicon wafer whose thickness is chosen to be $\sim\lambda/2$ (482.8 μm) at 90 GHz ($\ell_2 = 480$ μm in Fig. 2). The LEKID dimensions a, g, h, h_s, and b in Fig. 1 provide the admittances, Y_{stripsL} and Y_{stripsC}, related to inductive and capacitive effects, respectively, of the equivalent circuit model in Fig. 2(a). The strip width $2a$ and spacing g are chosen to provide the broadest bandwidth around 90 GHz with $Re(Y_{\text{stripsL}}) = 1/\eta_0$. The admittance of the short sections is obtained for two cases, strip width $2a$ and spacing h [Fig. 1(a)] and strip width b and spacing h_s [Fig. 1(b)]. The susceptance of the equivalent admittance ($Y_{\text{strips}} = Y_{\text{stripsL}} + Y_{\text{stripsC}}$) is compensated with a capacitive effect through an air gap ($\ell_1 = 970$ μm, $\sim 0.29\lambda$ at 90 GHz in Fig. 2) ending in a backshort to be optically matched to the free space, maximizing the absorption and bandwidth. The cross section of the structure is shown in Fig. 2(b), where $\varepsilon_{r\text{Air}}$ is 1.

For simulation purposes, a nominal Ti/Al sheet resistance of 1.27 Ω/sq is used; however, it is worth noting that this value may differ between the different experiments due to nanofabrication tolerances. With this value, the dimensions for the LEKIDs in Fig. 1 to match the air impedance are $a = 1.5$ μm and $g = 443$ μm. The calculated impedance of the long strips ($1/Y_{\text{stripsL}}$) at 90 GHz has an equivalent circuit composed of a 187.5-Ω resistance in series with a 403-pH inductor, whereas the equivalent circuit for the short section of the meandered line ($1/Y_{\text{stripsC}}$) is a capacitor of 0.0049 fF for the shape shown in Fig. 1(a) and 6 fF for the sawtooth shape [Fig. 1(b)].

For the analysis of an incident plane wave with horizontal E-field (TEM$_H$) referred to the position of the LEKID in Fig. 1, the different geometries of the short horizontal sections in Fig. 1(a) and (b) are taken into account. The impedance of the LEKID in Fig. 1(a) is calculated for strips of $2a$ width and spacing h of 3083 μm. On the other hand, for the sawtooth short sections, shown in Fig. 1(b), with sections of 15° angle separated by 30 μm, at the W-band, the impedance can be calculated like uniform strips of width b of 103.5 μm and spacing h_s of 2949 μm. Both impedances are obtained based on equations in [26] and [27] and the equivalent circuit of the calculated impedance for these short sections ($1/Y_{\text{stripsL}}$) at 90 GHz is a 1300-Ω resistance in series with a 4.42-nH inductor for the LEKID of Fig. 1(a), whereas for the sawtooth shape LEKID in Fig. 1(b), it is a 36-Ω resistance with a 1.97-nH inductor. The short sections with a less resistive impedance result in a structure with a greater free space mismatching and, therefore, in a lower absorption. The capacitive effect of the long strips ($1/Y_{\text{stripsC}}$) in both cases for this incident wave is 0.332 fF.

Subsequently, using these values for the equivalent circuit as a starting point, the optimization of the LEKID is obtained through 3-D EM simulations. They are carried out at the W-band for an infinite array of LEKIDs on 480-μm-thick silicon and the backshort with 970-μm air using unit cell analysis and a Floquet port with HFSS in Ansys Electronics Desktop [28]. Driven option Modal is selected as solution type for the analysis in HFSS, to compute incident plane waves. The initial mesh is smaller than 0.333λ and the maximum error is set to 0.01 for adaptive solution. From these 3-D EM simulations, it is found that the short parts of the inductive meander line are responsible for the absorption in the cross-polarization, which is calculated for each E-field polarization as $1-|S_{11}|^2$. Fig. 3 shows LEKID absorption results for HFSS simulation and circuit model simulation without an interdigital capacitor. The circuit models agree with the HFSS simulation results. A maximum absorption around 99% is predicted at 91 GHz depicted in Fig. 3(a), whereas an improvement for the cross-polarization with the sawtooth LEKID is obtained as shown in Fig. 3(b).

B. Low-Frequency Resonator Design

The proposed LEKID based on a series capacitor–inductor resonator is coupled to a 50-Ω CPW transmission line. The inductor geometry is fixed for the optical absorption, while other parameters such as capacitance and coupling need to be optimized. Momentum (Keysight Technologies) [29] and Sonnet [30] simulators are employed for this purpose.

First, an interdigitated capacitor of 0.7 pF is employed for fixing the readout resonant frequencies around 650 MHz and its value is swept from pixel to pixel by changing the length of one of its fingers for readout purposes.

Then, an accurate design of the coupling factor is critical for the dynamic range optimization of the detector under millimeter-wave radiation [31]. The loaded quality factor of the resonator, Q, is given by

$$\frac{1}{Q} = \frac{1}{Q_{\text{i}}} + \frac{1}{Q_{\text{c}}} \tag{1}$$

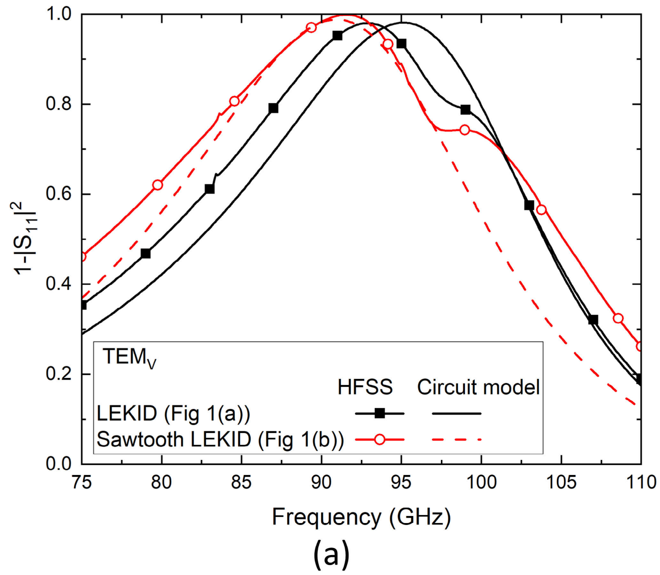

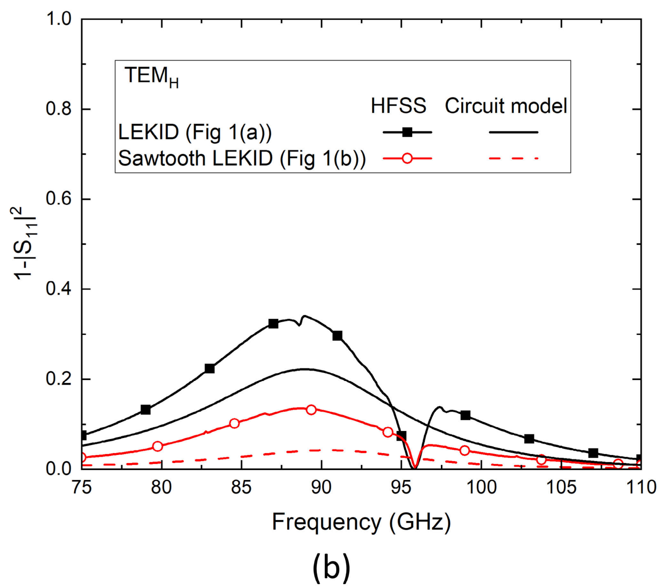

Fig. 3. LEKID absorption results for HFSS simulation and circuit model simulation without the interdigital capacitor. (a) Vertical E-field (TEM$_V$) referred to the position of the LEKIDs in Fig. 1. (b) Horizontal E-field (TEM$_H$) referred to the position of the LEKIDs in Fig. 1.

where the internal quality factor, Q_i, refers to the internal losses of the resonator, and the coupling quality factor, Q_c, describes the strength of the coupling to the transmission line. In our case, the expected Q_i under illumination is of the order of 10^5. A coupling factor $Q_c \approx 10^4$ is chosen to avoid the undercoupling regime ($Q_i < Q_c$), where the detector visibility (depth in the transmission scattering parameter, S_{21}) is degraded [4]. For this purpose, an inductive coupling of the LEKID to the CPW is made through one of the long sections of the meandered line and the distance between the LEKID and the ground plane (s_1) as well as the inner ground plane width (m) are optimized. These parameters of the LEKID design are depicted in Fig. 1, where $m = 40$ μm and $s_1 = 109$ μm.

III. LEKID Fabrication

The prototypes are fabricated by means of confocal sputtering following the technological process detailed in [25].

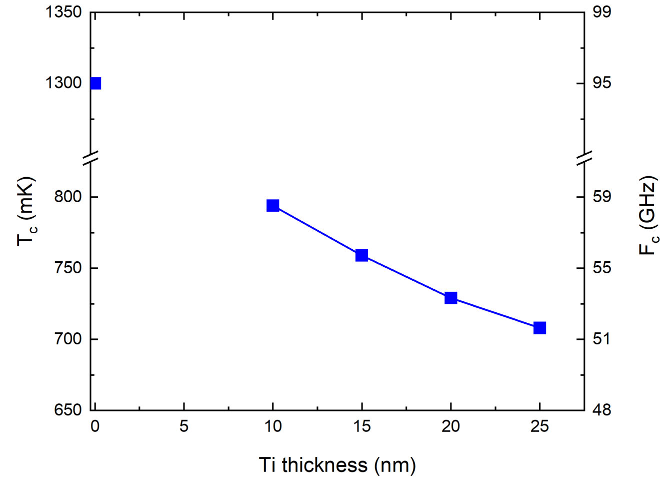

Fig. 4. Dependence of the critical temperature and cut-off frequency of the bilayer film with the titanium thickness over a 15-nm aluminum layer.

A. Tuning Cut-Off Frequency

The absorption capacity of a superconductor is limited by the energy required to break Cooper pairs, twice the superconducting gap, leading to a cut-off frequency, f_{cut}. The superconducting gap, Δ, is proportional to the critical temperature, T_c, according to $2\Delta \approx 3.52\ k_B T_c$, where k_B is the Boltzmann constant. In bulk aluminum, the critical temperature is 1.2 K that prevents the use of this material for detection in the W-band. However, the critical temperature can be reduced using the well-known superconducting proximity effect with a lower T_c superconductor, such as titanium (with a bulk critical temperature of 0.38 K), resulting in a bilayer film [32].

Superconducting critical temperature is characterized for several Ti/Al bilayers by cryogenic transport measurements. The Al thickness is fixed to 15 nm, whereas the Ti thickness is varied from 25 to 10 nm. As can be seen in Fig. 4, even though the aluminum layer has a critical temperature of 1.3 K, by increasing the Ti layer thickness in the bilayer film, it can be reduced down to 700 mK. This dependence on Ti thickness demonstrates that the larger the thickness of the Ti layer, the lower the effective T_c of the bilayer is [17]. Considering the bilayer film as a pure superconductor, this is directly translated into a cut-off frequency smaller than 60 GHz, making the superconducting resonators suitable for the W-band (75–110 GHz).

B. LEKID Demonstrators Nanofabrication

For the cryogenic characterization, a nine-element array demonstrator with the sawtooth strip is fabricated in a 15-nm Ti/15-nm Al bilayer on a high-resistive silicon 480-μm-thick wafer with a measured T_c of 785 mK. A photograph of the fabricated device is shown in Fig. 5.

Two dedicated prototypes for each LEKID design are fabricated to measure their absorption at room temperature using the quasi-optical setup described in [23]. These measurements allow us to validate the design and extrapolate the absorption to low-temperature conditions. All of them are based on a

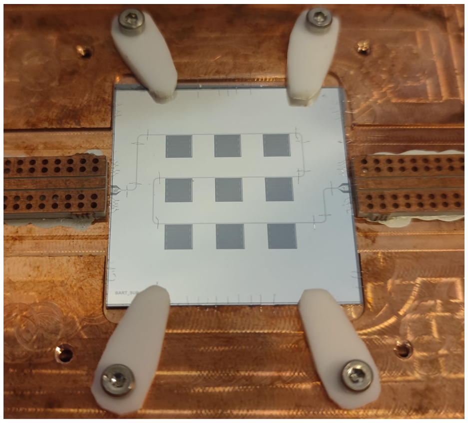

Fig. 5. Photograph of 3 × 3 LEKID prototype mounted for cryogenic characterization (wafer size 30 × 30 mm).

conducting film on a 480-μm silicon wafer. A 39-nm-thick aluminum layer with sheet resistance $R_s = 1.03\ \Omega/\text{sq}$ is used as conducting film to match the sheet resistance to the one expected for the Ti/Al bilayer at cryogenic temperature. As mentioned before, the sheet resistance value differs from the one used in the design stage since it depends on the fabrication run due to nanofabrication tolerances. The first two demonstrator versions consist of an 11 × 11 LEKID array with a total size of 40 × 40 mm, which includes both the inductor, straight and sawtooth shapes, and the capacitor of the LEKID structure [see a photograph of the sawtooth-LEKID design demonstrator in Fig. 6(a) and (b)]. Two extra prototypes with only the inductor structures (without the interdigital capacitors) are also manufactured for cross-polarization studies [see Fig. 6(c)].

IV. Experimental Setup

A. Room-Temperature Test System

For the room-temperature characterization, a quasi-optical system based on a free-space measurement is used. The system consists of two horn antennas, two dielectric lenses to collimate the beam at the measurement plane, and a vector network analyzer as explained in [23]. The feed antenna shows wide bandwidth and excellent cross-polarization, allowing an almost perfect plane wave with only one polarization. Rectangular waveguide antennas, model QSH-SL-75-110-F-20 from Steatite, are employed, providing around 20-dBi gain with dimensions $a \times b = 14.8 \times 11$ mm at the aperture. The calculated output beam waist radius, at the reference plane of the array under measurement, is 16.87 mm, which establishes the size of the array's samples under measurement to a minimum diameter of around 34 mm for its correct characterization as an infinite array [23].

B. Cryogenic Test System

For the cryogenic characterization, a dilution He3/He4 refrigerator (Bluefors LD-250) is employed. The cryogenic harness is composed of CuNi and NbTi radio-frequency lines, attenuators, dc blocks, and a low-noise amplifier in the 4-K stage. The readout setup is based on LNA and a vector network analyzer E5071C (VNA). Further information is included in [23].

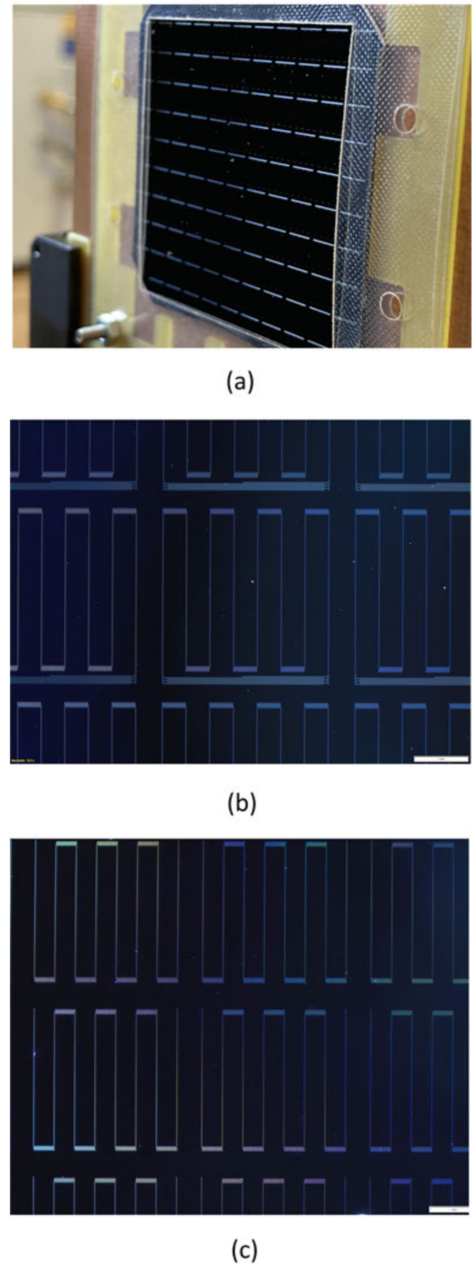

Fig. 6. Fabricated array of 11 × 11 LEKIDs with sawtooth inductor on a 480-μm silicon wafer. (a) LEKID array assembly to be characterized at room temperature with size 40 × 40 mm. (b) Detail of the first prototype (LEKIDs with an inductor and a capacitor). (c) Detail of the second prototype (LEKIDs without capacitor).

A dedicated holder, shown in Fig. 7, is designed to anchor the LEKID demonstrator to the 10-mK cold plate and assembles the required stack of optical elements to properly configure the experiments. The main chassis consists of a copper box where a 30 × 30 mm^2 area is drilled in the center of the package to place the demonstrator. It enables the connection of the chip with the cryogenic harness through circuit printed boards and SMA connectors. On top of it, there is an aperture lid that limits the incoming radiation to the center pixel, and two supports hold a 110-GHz cut-off frequency

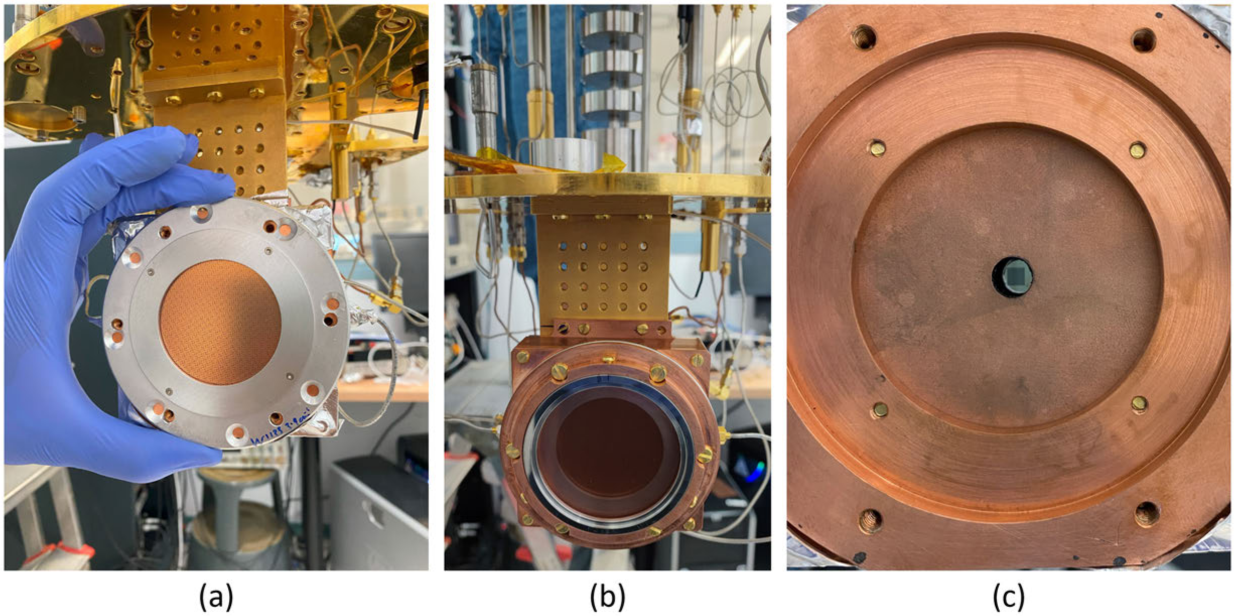

Fig. 7. Cryogenic experimental setup for the optical characterization. (a) W-band low-pass filter. (b) Assembly of the holder in the millikelvin stage with the polarizer on top. (c) Details of the aperture lid placed over the center LEKID.

low-pass filter and a linear polarizer. On the rear part, a copper backshort is placed at 970-μm distance from the sample backside for optical matching. An absorber material suitable for the W-band based on Stycast 2850 FT is used to cover the inner metal parts of the holder. For responsivity analysis, a blackbody load, provided with a temperature controller, is installed at the 4-K stage.

In addition, a spectroscopic cryogenic characterization of a single pixel is performed. The measurement setup consists of an SMB100A signal generator together with an SMZ110 frequency multiplier, both from Rohde&Schwarz that generate the W-band signal, and a W-band antenna (model 27240-20 from Flann Microwave) that defines the orientation of the E-field at room temperature and it is used to illuminate the array. Teflon-based lenses, infrared filters, and a 110-GHz low-pass filter are assembled in the different cryostat stages. Further details of the employed system are explained in [33].

V. Experimental Results

A. Room-Temperature Measurements

First, the room-temperature prototypes based on the complete LEKIDs (with capacitors and inductors), described in Section III-B are characterized for the two orthogonal linearly polarized waves in the 75–110-GHz frequency range with the quasi-optical test bench. Fig. 8 shows the simulated and measured absorption of the LEKIDs for a linearly polarized incident wave parallel and perpendicular to the LEKID inductor at room temperature.

For both prototypes, the response to the vertical illumination (TEM$_V$) demonstrates a maximum absorption of around 94% at 92 GHz. The absorption in the frequency band can be affected by several issues, such as the thickness of the wafer, the air gap, and the thickness or sheet resistance of the bilayer. A sensitivity analysis, starting at nominal values for all these parameters, is carried out considering the fabrication tolerances, shown in Fig. 8. The parameters taken into account in the analysis are silicon thickness 480 $\pm$ 10 μm, the air gap to the backshort 970 $\pm$ 10 μm, and the film thickness 39 $\pm$ 3 nm ($R_s = 1.16{-}0.99$ Ω/sq). Taking into account these tolerances, a good agreement between measurements and simulations for a TEM$_V$ wave is obtained. However, the absorption for the TEM$_H$ wave results in an undesired high reflection coefficient in both cases. As obtained from the circuit model and the 3-D simulations, this is mainly due to the interdigital capacitors. In this case, slight discrepancies between simulation and measurement are obtained which can be attributed to a small misalignment of the array in the quasi-optical measurement setup, or even edge effects.

To demonstrate the cross-polarization improvement for the new sawtooth design, the second manufactured arrays including just inductors are characterized. The comparison between both designs, shown in Fig. 9, confirms the reduction of the undesired component using the new sawtooth topology and the effect caused by the capacitor depicted in Fig. 8 is removed. Moreover, for all fabricated prototypes the measured absorption versus frequency for the TEM$_V$ shows almost the same response. It is worth noting that at cryogenics conditions, the absorption in the capacitor has no impact since photons hitting the capacitor will not be detected as no change in the kinetic inductance (L_k) will be produced [34].

B. Cryogenic Temperature Measurements

The previously presented single-polarization array of nine LEKIDs with the sawtooth inductor is characterized at cryogenic conditions using the setup shown in Section IV-B.

1) Dark Characterization: The holder is fully enclosed using a copper lid and aluminum foil, to avoid any undesired radiation exciting the LEKIDs. Using the VNA, a frequency

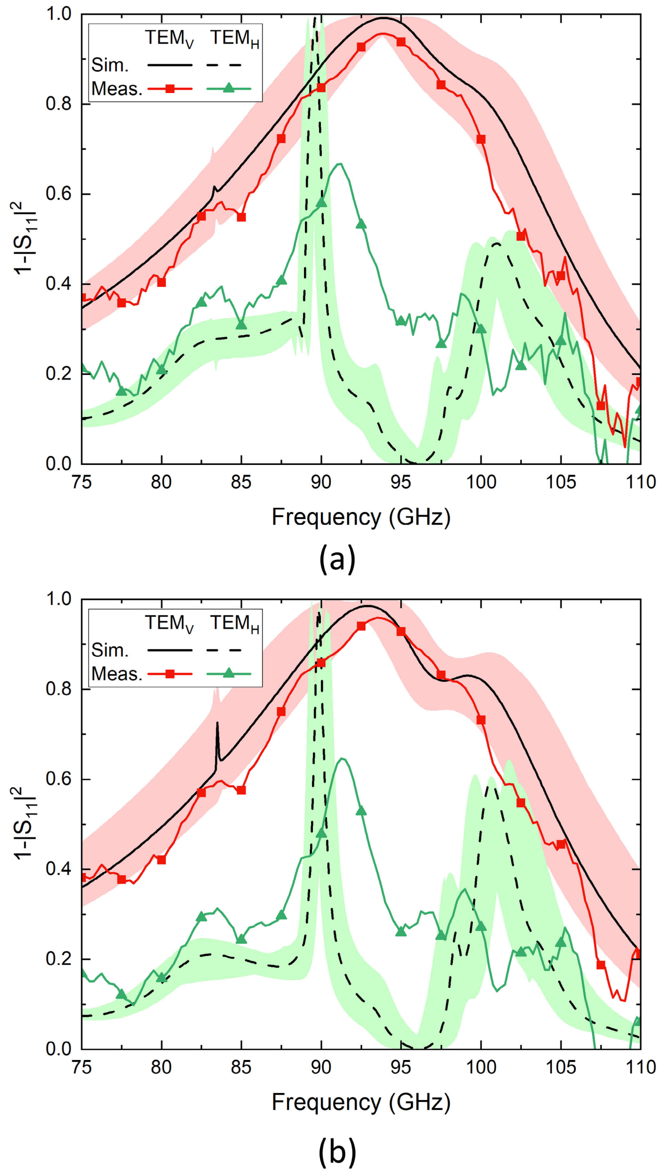

Fig. 8. Simulated and measured absorption at room temperature for the 39-nm aluminum LEKID ($R_s = 1.03\ \Omega/\text{sq}$) on the silicon wafer. Linearly polarized incident wave for orthogonal polarizations. Sensitivity analysis (shaded areas). Silicon thickness 480 $\pm$ 10 μm, air gap to the backshort 970 $\pm$ 10 μm, and film thickness 39 $\pm$ 3 nm ($R_s = 1.16$–$0.99\ \Omega/\text{sq}$). (a) LEKIDs in Fig. 1(a). (b) Sawtooth LEKIDs in Fig. 1(b).

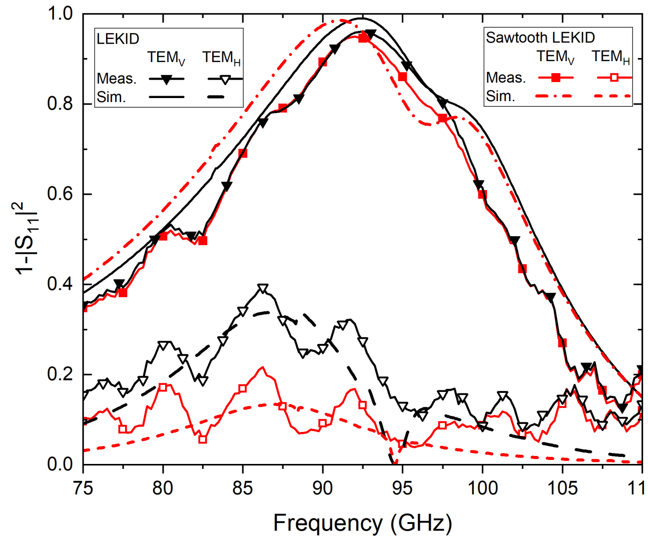

Fig. 9. Simulated and measured absorption at room temperature for the LEKID prototypes without capacitors. Linearly polarized incident wave for orthogonal polarizations.

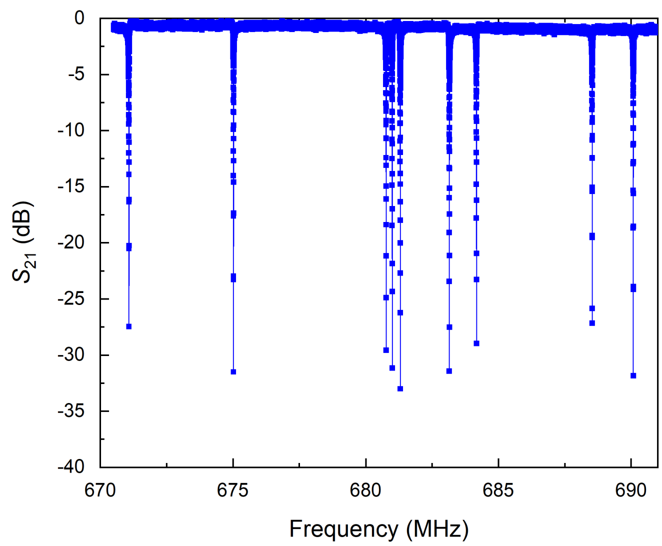

Fig. 10. Resonant frequencies for the fabricated 3×3 LEKID array with the sawtooth strip, under dark conditions at $T = 10$ mK, with an input power at the detector of $P_{\text{in}} = -105$ dBm and a frequency step 1.025 kHz.

sweep is performed to individually characterize the resonant frequency and the quality factor of each resonator. A transmission response calibration is performed to set the reference plane of the measurement, correcting the input and output paths up to the LEKIDs plane. This procedure is done at 700 mK, just below the superconducting transition where LEKIDs are still not visible [31]. Fig. 10 shows the obtained forward scattering parameter (S_{21}) amplitude at 10 mK with an input power $P_{\text{in}} = -105$ dBm in the detector, setting the VNA with a power of $P_{\text{VNA}} = -75$ dBm, a frequency range from 670.5 to 691.0 MHz, and a frequency step of 1.025 kHz. Nine dips are observed, corresponding to each one of the nine fabricated LEKIDs. By varying the capacitance, the resonators are designed for having resonant frequencies 3 MHz step. However, the obtained resonant frequencies are nonhomogeneously spaced due to fabrication tolerances. From the obtained resonant frequency, the kinetic inductance L_k and kinetic inductance fraction, α, are estimated as follows. First, the LEKID made of a lossless metal and $L_k = 0$ is simulated using the Sonnet EM simulator, obtaining the values for the geometrical inductance ($L_g = 36$ nH) and capacitance ($C \approx 0.7$ pF). From these values and the experimental resonant frequency ($f_{\text{res}} = 1/(2\pi((L_g+L_k)C)^{1/2})$), the kinetic inductance is extracted and the kinetic fraction is calculated as $\alpha = (L_k/L_g + L_k)$, obtaining $L_k = 2.86$ pH/sq and $\alpha = 0.53$ [16].

Fig. 11 shows the quality factor of each resonator obtained by following the procedure detailed in [35]. Coupling quality factors around $2 \cdot 10^4$ are obtained, which match reasonably

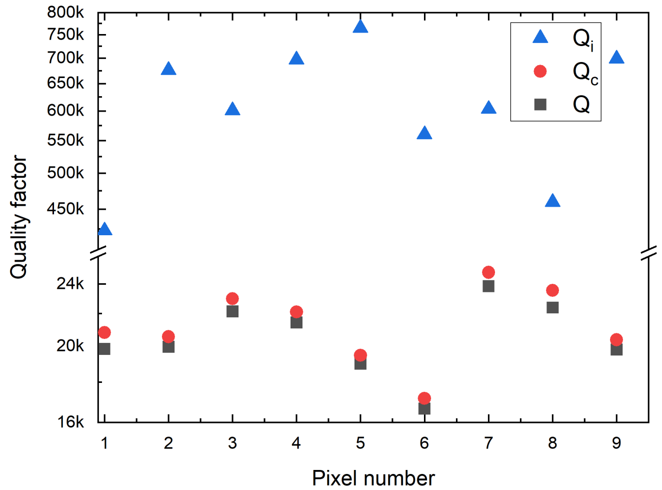

Fig. 11. Quality factors for the nine fabricated pixels under dark conditions at $T = 10$ mK. Q is the loaded quality factor, Q_i the internal quality factor, and Q_c the coupled quality factor. Values obtained from the frequency sweep in Fig. 10.

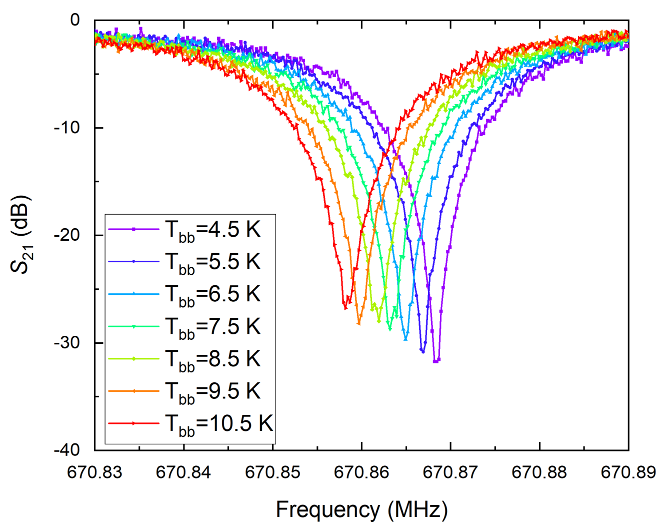

Fig. 12. Transmission measurement corresponding to the illuminated LEKID as a function of blackbody temperature (T_{bb}). The radiation linear polarization is parallel to the inductor lines.

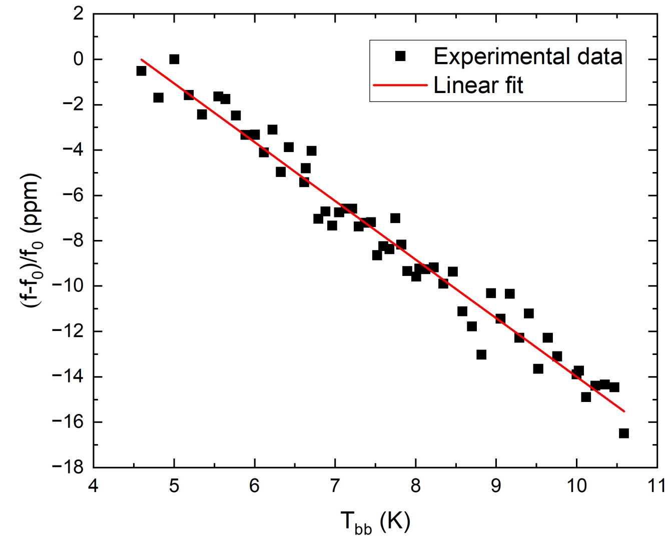

Fig. 13. Temperature dependence of the optical responsivity of the illuminated LEKID, with fitting parameters: $r^2 = 0.96661$, $\chi^2 = -0.98316$, and RMSE = 0.61627.

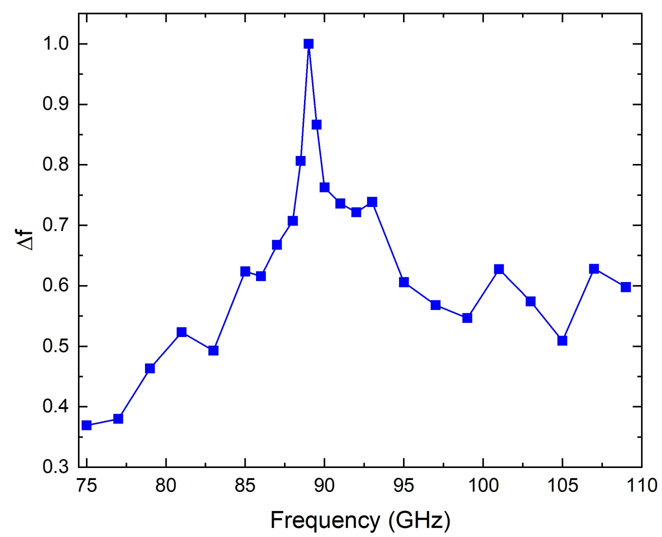

Fig. 14. Frequency shift of the resonant frequency with respect to the one in darkness condition (f_{off}) normalized to its maximum value (f_{off}−f_{illum}) as a function of the input radiation frequency within the W-band.

well to the designed values. In addition, internal quality factors greater than $6 \cdot 10^5$ demonstrate the good quality of the fabricated films.

2) Responsivity Characterization: For optical characterization, the holder faces the blackbody load, and the lid of the holder is replaced by the aperture lid, filter, and polarizer, presented in Section IV-B. The polarizer is aligned with the inductor lines to fix the polarization of the incoming radiation. The blackbody temperature (T_{bb}) is swept from 4.5 to 10.5 K, increasing the optical power. The results are shown in Fig. 12 where the shift to lower frequency and the decrease in the quality factor confirm the response to the incoming radiation.

The fractional frequency shift is defined as

$$x = \frac{(f - f_0)}{f_0} \tag{2}$$

where f_0 and f are the initial measured frequency and the measured frequencies, respectively. In Fig. 13, this frequency shift is plotted as a function of the blackbody temperature. A linear relationship is observed, corresponding to the slope, $\partial x/\partial T_{bb}$, to the detector responsivity which is 2.58 ppm/K, agreeing with previous experiments [12].

3) Spectroscopic Characterization: The spectral responsivity of the detectors is characterized using the external W-band setup previously explained in Section IV-B and consists in the study of the relative shift of the resonant frequency of the LEKID normalized to its maximum value, given by

$$\Delta f = (f_{\text{off}} - f_{\text{illum}})/\max(f_{\text{off}} - f_{\text{illum}}) \tag{3}$$

where f_{off} is the resonant frequency in dark conditions and f_{illum} is the measured resonant frequencies as a function of the frequency of the incoming radiated signal. Fig. 14 shows the obtained results which confirm the response within the W-band using the Ti/Al technology and the optical design. A maximum shift in the resonant frequency is observed around 90 GHz demonstrating the high-frequency quasi-optical design and agrees with the room-temperature results.

VI. Conclusion

In this work, we present an improved state-of-the-art design of superconducting LEKIDs for future astronomical experiments in the W-band. In LEKIDs, the inductor, which acts as the sensing area of the detector, consists of parallel vertical lines joined by short horizontal sections that cause a nondesired orthogonal absorption and, hence, induce cross-polarization. Based on equivalent circuits and 3-D EM simulations, we demonstrate that this undesired cross-polarization absorption can be reduced by engineering the short horizontal section admittances. A sawtooth-based structure LEKID is proposed for reducing the sensitivity in the undesired direction. Room-temperature optical characterization shows a reduction of the cross-polarization when compared with traditional LEKIDs. A nine-pixel prototype is tested at cryogenic temperature, demonstrating sensitivity in the W-band. This design pushes forward the previous efforts for developing on-chip polarimeters based on LEKIDs and opens the possibility of its use in polarimetric astronomical experiments in the W-band.

Acknowledgment

The authors would like to thank Eva María Cuerno and Paul García with the Departmento de Ingeniería de Comunicaciones, Universidad de Cantabria, Santander, Spain, for the fabrication of the printed circuit boards. They would also like to thank Ricardo Ferrándiz with the Centro de Astrobiología (CSIC-INTA), Madrid, Spain, for holder design and mechanical assemblies. They would also thank IMDEA-Nanociencia, Madrid, cleanroom staff for support in samples nanofabrication.

References

[1] B. Aja et al., "The canfranc axion detection experiment (CADEx): Search for axions at 90 GHz with kinetic inductance detectors," *J. Cosmol. Astroparticle Phys.*, vol. 2022, no. 11, p. 044, Nov. 2022.

[2] K. Lee et al., "GroundBIRD: A CMB polarization experiment with MKID arrays," *J. Low Temp. Phys.*, vol. 200, nos. 5–6, pp. 384–391, Sep. 2020.

[3] J. G. Bartlett, "Cosmic microwave background polarization," *J. Phys., Conf.*, vol. 39, no. 1, pp. 1–8, Sep. 2006.

[4] A. Paiella et al., "Total power horn-coupled 150 GHz LEKID array for space applications," *J. Cosmol. Astroparticle Phys.*, vol. 2022, no. 6, p. 009, Jun. 2022.

[5] Y.-H. Kim, S.-J. Lee, and B. Yang, "Superconducting detectors for rare event searches in experimental astroparticle physics," *Superconductor Sci. Technol.*, vol. 35, no. 6, Jun. 2022, Art. no. 063001.

[6] J. Zmuidzinas and P. L. Richards, "Superconducting detectors and mixers for millimeter and submillimeter astrophysics," *Proc. IEEE*, vol. 92, no. 10, pp. 1597–1616, Oct. 2004.

[7] K. Hattori et al., "Development of superconducting detectors for measurements of cosmic microwave background," *Phys. Proc.*, vol. 37, pp. 1406–1412, Jan. 2012.

[8] M. Calvo et al., "Improved mm-wave photometry for kinetic inductance detectors," *Astron. Astrophys.*, vol. 551, p. 12, Mar. 2013.

[9] A. Monfardini et al., "NIKA: A millimeter-wave kinetic inductance camera," *Astron. Astrophys.*, vol. 521, p. 29, Oct. 2010.

[10] M. Roesch et al., "Development of lumped element kinetic inductance detectors for NIKA," in *Proc. 22nd Int. Symp. Space Terahertz Technol.*, Apr. 2011, pp. 41–45.

[11] J. van Rantwijk, M. Grim, D. van Loon, S. Yates, A. Baryshev, and J. Baselmans, "Multiplexed readout for 1000-pixel arrays of microwave kinetic inductance detectors," *IEEE Trans. Microw. Theory Techn.*, vol. 64, no. 6, pp. 1876–1883, Jun. 2016.

[12] H. McCarrick et al., "Design and performance of dual-polarization lumped-element kinetic inductance detectors for millimeter-wave polarimetry," *Astron. Astrophys.*, vol. 610, p. 45, Feb. 2018.

[13] L. Perotto et al., "Calibration and performance of the NIKA2 camera at the IRAM 30-m telescope," *Astron. Astrophys.*, vol. 637, p. 71, May 2020.

[14] A. Paiella et al., "Kinetic inductance detectors for the OLIMPO experiment: Design and pre-flight characterization," *J. Cosmol. Astroparticle Phys.*, vol. 2019, no. 1, p. 039, Jan. 2019.

[15] P. K. Day, H. G. LeDuc, B. A. Mazin, A. Vayonakis, and J. Zmuidzinas, "A broadband superconducting detector suitable for use in large arrays," *Nature*, vol. 425, no. 6960, pp. 817–821, Oct. 2003.

[16] S. Doyle, "Lumped element kinetic inductance detectors," Ph.D. dissertation, School Phys. Astron., Cardiff Univ., Wales, U.K., Apr. 2008.

[17] A. Catalano et al., "Bi-layer kinetic inductance detectors for space observations between 80–120 GHz," *Astron. Astrophys.*, vol. 580, p. 15, Aug. 2015.

[18] A. Catalano et al., "Maturity of lumped element kinetic inductance detectors for space-borne instruments in the range between 80 and 180 GHz," *Astron. Astrophys.*, vol. 592, p. 26, Aug. 2016.

[19] A. Catalano et al., "Sensitivity of LEKID for space applications between 80 GHz and 600 GHz," *Astron. Astrophys.*, vol. 641, p. 179, Sep. 2020.

[20] S. Shu et al., "Development of octave-band planar ortho-mode transducer with kinetic inductance detector for LiteBIRD," *Proc. SPIE*, vol. 9914, pp. 577–582, Jul. 2016.

[21] Q. Y. Tang, P. S. Barry, T. W. Cecil, and E. Shirokoff, "Fabrication of OMT-coupled kinetic inductance detector for CMB detection," *J. Low Temp. Phys.*, vol. 199, nos. 1–2, pp. 362–368, Apr. 2020.

[22] J. Perido et al., "Extending KIDs to the mid-IR for future space and suborbital observatories," *J. Low Temp. Phys.*, vol. 199, nos. 3–4, pp. 696–703, May 2020.

[23] B. Aja et al., "Analysis and performance of lumped-element kinetic inductance detectors for W-band," *IEEE Trans. Microw. Theory Techn.*, vol. 69, no. 1, pp. 578–589, Jan. 2021.

[24] M. C. de Ory et al., "Development of W-band dual-polarization kinetic inductance detectors on silicon," in *IEEE MTT-S Int. Microw. Symp. Dig.*, Jun. 2023, pp. 570–573.

[25] B. Aja et al., "Bi-layer kinetic inductance detectors for W-band," in *IEEE MTT-S Int. Microw. Symp. Dig.*, Aug. 2020, pp. 932–935.

[26] N. Marcuvitz, "Gratings and arrays in free space," in *Waveguide Handbook*. New York, NY, USA: McGraw-Hill, 1951, pp. 280–285.

[27] R. Ulrich, "Far-infrared properties of metallic mesh and its complementary structure," *Infr. Phys.*, vol. 7, no. 1, pp. 37–55, Mar. 1967.

[28] *ANSYS HFSS Software*. Accessed: Jun. 16, 2023. [Online]. Available: http://www.ansoft.com/products/hf/hfss/

[29] *ADS Software*. Accessed: Jun. 16, 2023. [Online]. Available: https://www.keysight.com/us/en/products/software/pathwave-design-software/pathwave-advanced-design-system.html

[30] Sonnet Software. *Sonnet User's Guide, Release 18*. Accessed: Jun. 16, 2023. [Online]. Available: https://www.sonnetsoftware.com/support/

[31] J. Zmuidzinas, "Superconducting microresonators: Physics and applications," *Annu. Rev. Condens. Matter Phys.*, vol. 3, no. 1, pp. 169–214, Mar. 2012.

[32] M. Tinkham, *Introduction to Superconductivity*. Chelmsford, MA, USA: Courier Corporation, 2004.

[33] D. Arrazola et al., "Optomechanical design for optical performance characterization of W-band kinetic inductance detectors," *J. Low Temp. Phys.*, vol. 209, nos. 5–6, pp. 1226–1231, Dec. 2022.

[34] D. Marsden et al., "Optical lumped element microwave kinetic inductance detectors," *Proc. SPIE*, vol. 8453, pp. 62–70, Sep. 2012.

[35] S. Probst, F. B. Song, P. A. Bushev, A. V. Ustinov, and M. Weides, "Efficient and robust analysis of complex scattering data under noise in microwave resonators," *Rev. Sci. Instrum.*, vol. 86, no. 2, Feb. 2015, Art. no. 024706. [Online]. Available: https://pubs.aip.org/aip/rsi/article/360955

Marina C. de Ory was born in Seville, Spain, in 1994. She received the Bachelor of Science and Material Engineering degree from Seville University, Seville, in 2017, and the Master of Nanoscience and Advanced Materials degree from Universidad Complutense de Madrid, Madrid, Spain, in 2018. She is currently pursuing the Ph.D. degree in the field of low-temperature physics, ultrasensitive detectors for astronomy, and quantum technologies at the Centro de Astrobiología (CSIC-INTA), Madrid.

She joined the Department of Transport and Quantum Phenomena, Complutense University of Madrid, as a Research Assistant, in 2018, where she was involved in superconductor transport measurements. Then, she joined Centro de Astrobiología (CSIC-INTA) in collaboration with IMDEA-Nanoscience, Madrid. Her research interests lie in the area of superconducting resonators, including modeling, nanofabrication, and low-temperature microwave characterization of microwave devices with applications in astrophysics and quantum computing. She is also involved in the study of the interaction of superconductors with 2-D and magnetic materials. She collaborates actively with other researchers in the same field and contributes to several scientific conferences.

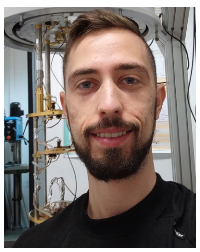

David Rodriguez was born in Zamora, Spain, in 1996. He received the B.Sc. degree in physics and the M.Sc. degree in condensed matter physics from the Universidad Autónoma de Madrid, Madrid, Spain, in 2018 and 2019, respectively. He is currently pursuing the Ph.D. degree in the field of superconducting circuits for quantum technologies and quantum sensing at the Centro de Astrobiología (CSIC-INTA), Madrid, under the supervision of Alicia Gomez.

During his B.Sc. degree, he joined the Department of Condensed Matter Physics, Universidad Autónoma de Madrid, as a Research Assistant, where he was involved in quantum transport measurements. He later joined the Advanced Nanomaterials and Devices, Technical University of Eindhoven, Eindhoven, The Netherlands, to conduct his master's thesis. In 2021, he joined Alicia Gomez's Group, as a Research Assistant and later became a Ph.D. student. His research focuses on the design of superconducting resonators for quantum and space applications. He is also involved in the development and control of qubits in collaboration with INMA-Universidad de Zaragoza, Zaragoza, Spain.

Enrique Villa was born in Santander, Spain. He received the bachelor's degree in telecommunications engineering, the master's degree in information technologies and mobile network communications, and the Ph.D. degree from the University of Cantabria, Santander, Spain, in 2005, 2008, and 2014, respectively.

From 2006 to 2017, he was a Researcher with the University of Cantabria, where he participated in the design of low-noise, high-sensitivity, and broadband microwave receivers for radio astronomy. He participated in the development of the QUIJOTE (Q-U-I JOint Tenerife) telescopes, dedicated to the analysis of the cosmic microwave background (CMB) in the frequency range from 10 to 47 GHz. He was a Visiting Researcher at the Instituto de Astrofísica de Canarias, Tenerife, Spain, during these years. In 2018, he was a Researcher with the Instituto de Astrofísica de Canarias, leading the development of microwave receivers for biomedical applications to measure the natural electromagnetic radiation of biological tissues. He participated in an international network focused on developing open-source medical software (3-D Slicer with MIT-Harvard and NA-MIC Project). He joined Centro de Astrobiología (CSIC-INTA), Madrid, Spain, in April 2022, where his main tasks are related to the development of state-of-the-art superconducting detectors for space missions and ground-based telescopes, designing microwave devices for the read-out system of superconducting detectors.

Dr. Villa was awarded with the extraordinary Ph.D. Prize in the Architecture and Engineering Area in 2016.

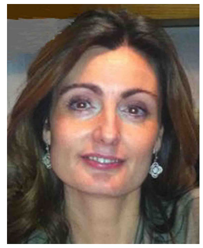

Luisa de la Fuente (Member, IEEE) received the M.Sc. degree in physics and the Ph.D. degree in electronic engineering from the University of Cantabria, Santander, Spain, in 1991 and 1997, respectively.

In 1992, she joined the Department of Communications Engineering, University of Cantabria, where she is currently an Associate Professor. In the past years, she has worked on projects focused on the development of radiometers for space applications, like the Planck Mission, in particular, in low-noise amplifiers at room and cryogenic temperatures, as well as in polarimetric receivers for radio astronomy applications in the frequency bands from 20 to 100 GHz for the QUIJOTE Project, installed in "El Teide Observatory" (Tenerife, Canary Islands). Currently, she is involved in several projects focused on the development of polarimeter detectors for the cosmic microwave background (CMB), based on kinetic inductance detectors (KIDs) in the *W* band. Her research interests include the design and characterization of low-noise amplifiers for cryogenic applications and radio astronomy receivers.

Beatriz Aja received the degree in telecommunications engineering and the Ph.D. degree from the University of Cantabria, Santander, Spain, in 1999 and 2007, respectively.

From 2008 to 2012 and from 2013 to 2015, she was an Invited Scientist at the Fraunhofer Institute for Applied Solid State Physics, Freiburg, Germany, in a joint collaboration project with Centro Astronómico de Yebes, Guadalajara, Spain, where her main activity was the design of monolithic microwave integrated circuits (MMIC) for cryogenic applications. She is currently an Associate Professor with the Department of Communications Engineering, University of Cantabria. Her research interests include the design and characterization of LNAs for cryogenic applications, superconducting kinetic inductance detectors and microwave and millimeter-wave passive components, and radio astronomy receivers.

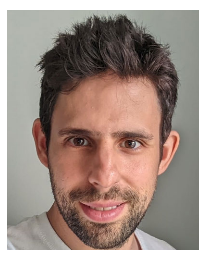

Victor Rollano was born in Madrid, Spain, in 1988. He received the B.Sc. and M.Sc. degrees in physics from the Universidad Complutense de Madrid, Madrid, Spain, in 2014 and 2015, respectively, and the Ph.D. degree from the Universidad Complutense of Madrid and IMDEA Nanoscience, Madrid, in 2019.

From 2020 to 2021, he joined the Quantum Materials and Devices Group, Instituto de Nanociencia y Materiales de Aragón (CSIC), Zaragoza, Spain, as a Post-Doctoral Researcher. During this period, his research was focused on settling the basis for the development of quantum processing units based on molecular spins. During his stage as a Ph.D. candidate, his research was focused on superconducting vortex dynamics on variable potentials created by magnetic or superconducting nanostructures.

Dr. Rollano was awarded the Margarita Salas Fellowship in 2021 and the Marie Skłodowska-Curie Fellowship in 2022 for the development of hybrid devices based on nitrogen-vacancy ensembles in diamond and superconducting qubits working at the Hybrid Quantum Devices Group, University of Science and Technology of China (USTC), Hefei, China.

María Teresa Magaz was born in Madrid, Spain, in 1965. She received the B.Sc. and M.Sc. degrees in organic chemistry and occupational health and safety from Universidad Autónoma de Madrid, Madrid, in 1986, 1988, and 2010, respectively.

From 2010 to 2015, she was a Research Assistant Technician in La Mara osa Campus, Institute of Technology (INTA), Madrid, working on optical photolithography for the development of PbSe IR detectors. Since 2017, she has been working as a Research Assistant Technician at the Centro de Astrobiología (CSIC-INTA) in collaboration with IMDEA-Nanociencia, Madrid. Her research focuses on the processing and optimization of nano- and microfabrication of ultrasensitive detectors for astronomy and quantum technologies. Her expertise includes sputtering and e-beam evaporation deposition in high vacuum conditions, dielectric deposition using atomic layer deposition (ALD), optical and electrical lithography, wet and dry etching techniques, and fabrication characterization.

Juan P. Pascual (Senior Member, IEEE) was born in Santander, Spain, in 1968. He received the M.Sc. degree (Hons.) in physics (specializing in electronics) and the Ph.D. degree in electronic engineering from the University of Cantabria, Santander, in 1990 and 1996, respectively.

He is currently an Associate Professor with the Communications Engineering Department, University of Cantabria, teaching analog and digital signal processing, RF and microwave design, monolithic microwave integrated circuits (MMICs) technologies, and telecommunications infrastructures. He has been involved in modeling and design projects with institutions like Alcatel Espacio, Tres Cantos, Madrid, Spain; OMMIC, Limeil Brevannes, France; ESA, ESTEC Noordwijk, The Netherlands; Technical University of Darmstadt, Darmstadt, Germany (where he stayed during 1999), the PLANCK, the QUIJOTE Mission, and the "Terahertz Technology for Electromagnetic Sensing Applications" (TERASENSE) Consortiums. He has participated in the Spanish Network of Excellence in Terahertz and has been responsible for a training program of Doctors for the industry (University of Cantabria-Erzia Tech., Santander). He has coauthored more than 80 contributions in journals and congress. His research interests are active device modeling, MMIC design methodologies of nonlinear functions and subsystems, from microwaves to millimeter waves and sensors in the THz bands, particularly for W band imaging systems and complex system simulation.

Daniel Granados received the Ph.D. degree in physical sciences from the Autonomous University of Madrid (UAM), Madrid, Spain, in 2006.

He is the Executive Director of Scientific Infrastructures, Madrilenian Institute for Advanced Studies in Nanoscience (IMDEA Nano), Madrid, and the Head of the Quantum NanoDevices Group. He is a Physicist at UAM. He completed his experimental doctoral studies at the Institute of Microelectronics in Madrid, which is part of the National Microelectronics Center of the Spanish National Research Council (IMN-CNM-CSIC). For three years, he was a Researcher at the Quantum Information Group, Toshiba Research Europe Ltd., Cambridge, U.K., and the Leader of the Photonic Confinement Group. He joined IMDEA-Nano in 2009 as the Head and Coordinator of Nanofabrication Services. He is the Vice-President of the Electronic Materials Division, International Union for Vacuum Science, Technique, and Applications (IUVSTA).

Dr. Granados is the Scientific Advisory Committee Member of the Spanish Vacuum Association (ASEVA). Since 2021, he has been the Executive Committee Member of the Circle Foundation for Security and Defense Technologies. Since 2022, he has served as a Scientific/Technical Advisor to the General Directorate for Research and Technological Innovation of the Community of Madrid for the PERTE-CHIP, and the Expert Committee Member of the Think Tank Future Trends Forum of the Bankinter Innovation Foundation. He contributed to the creation and launch of the Madrid Cluster for Innovation, Technology, and Talent in Semiconductors of the Community of Madrid and has been its director since January 2023.

Eduardo Artal (Life Member, IEEE) received the degree and Dr.-Eng. degree in telecommunication engineering from the Technical University of Catalonia, Barcelona, Spain, in 1976 and 1982, respectively.

From 1976 to 1990, he was an Assistant Professor with the Technical University of Catalonia. From 1979 to 1981, in a partial leave from the university, he joined Mier Allende S.A., Barcelona, working on TV and FM radio re-emitters development. Since 1990, he has been a Professor at the University of Cantabria, Santander, Spain. His current research interests include microwave circuits and low-noise millimeter-wave amplifiers and receivers for radio astronomy.

Alicia Gomez was born in Madrid, Spain, in 1986. She received the B.Sc. and M.Sc. degrees in physics from the Universidad Complutense de Madrid, Madrid, in 2009 and 2010, respectively, and the Ph.D. degree from Universidad Complutense of Madrid, in 2013, with a focus on superconducting vortex dynamics.

She was a Visiting Researcher at the University of California, Davis, Davis, CA, USA, in 2010; and the University of Antwerp, Antwerp, Belgium, in 2012. Since 2013, she has been the Group Leader of the Superconducting Technologies Group, Centro de Astrobiología (CSIC-INTA), Madrid, for the development of superconducting circuits for space and quantum applications. Her experience spans from the design and nanofabrication of superconducting electronics in cleanrooms to the electronic characterization of superconducting devices at cryogenic temperatures with and without magnetic fields. She works on the development of kinetic inductance detectors (KIDs) for space and ground-based astrophysics instrumentation and has been part of international collaborations such as the NIKA2 Camera installed at the IRAM 30 m telescope in Granada, the KISS Camera for the Canary Island telescope and the CORE proposal submitted to the call for the M5 mission of the ESA Cosmic Vision. She is now leading the KIDs developments for the CADEx experiments in the search for dark matter. Recently, her work has spanned the development of optimized superconducting circuits to be implemented in a proof-of-concept of large-scale molecular spin quantum processors. She has been PI in seven projects and has contributed to more than 15. She has coauthored more than 50 peer-reviewed articles.